

Electronic Structures of Antiperovskite Superconductor MgCNi₃ and Related Compounds

J. H. SHIM,* S. K. KWON and B. I. MIN

Department of Physics, Pohang University of Science and Technology, Pohang 790-784, Korea

Electronic structure of a newly discovered antiperovskite superconductor MgCNi₃ is investigated by using the LMTO band method. The main contribution to the density of states (DOS) at the Fermi energy E_F comes from Ni 3*d* states which are hybridized with C 2*p* states. The DOS at E_F is varied substantially by the hole or electron doping due to the very high and narrow DOS peak located just below E_F . We have also explored electronic structures of C-site and Mg-site doped MgCNi₃ systems, and described the superconductivity in terms of the conventional phonon mechanism.

KEYWORDS: Antiperovskite, Superconductor, Electronic structure, MgCNi₃

§1. Introduction

In contrast to the ordinary perovskite structure, antiperovskite structure has metal elements at the corners of the octahedron cage. Ordinarily transition metal based antiperovskites have magnetic ground states. For example, Mn-based antiperovskites have been studied due to their complex magnetic structure¹⁾ and large magnetoresistance.^{2,3)} Recently, superconductivity is observed in antiperovskite MgCNi₃ with transition temperature of $T_c \sim 8$ K by He *et al.*⁴⁾ It is rather surprising that the superconductivity is observed in such materials with much Ni contents. Band calculations show that very narrow and high peak is located just below E_F in density of states (DOS) curve.^{5,7,6,8,9)} This peak has mainly Ni 3*d* character hybridized with C 2*p* states.⁷⁾

Superconductivity of MgC_{*x*}Ni₃ is very sensitive to the C contents *x*. It disappears in between $x = 0.96 \sim 0.90$.⁴⁾ By Ni-site doping, superconductivity is also suppressed either hole with Co or electron doping with Cu, respectively.⁵⁾ Especially, Co doping does not induce magnetism,¹⁰⁾ and so the magnetism is not the origin of suppression of the superconductivity. Hence the mechanism of abrupt quenching of superconductivity is not known yet. It is also expected that Mg-site hole doping will produce the magnetic ground state.^{8,9)}

In this work, we have explored C-site and Mg-site doping effects with substituting neighboring atoms in the periodic table. By comparing the DOS, Stoner factor, and electron phonon coupling constant, we have discussed the effect of doping on the superconductivity and magnetism.

§2. Computational details

We have used the linearized muffin-tin orbital (LMTO) band method in the local density approximation (LDA). The LMTO band calculation includes muffin-tin orbitals up to *d*-site for Mg, C, and up to *f*-site for Ni. We have considered a cubic structure with lattice constant $a =$

3.816 Å, which is for the highly stoichiometric MgCNi₃ with highest T_c .⁴⁾ Atomic positions are Mg at (0 0 0), C at (1/2 1/2 1/2), and Ni at (1/2 1/2 0), (1/2 0 1/2), and (0 1/2 1/2). Atomic sphere radii of Mg, C, and Ni are employed as 3.20, 1.54 and 2.49 Å, respectively. For the calculation of doped MgCNi₃ systems, we have considered a supercell with the doubled unit cell. One type of Mg or C (111) planes alternate with other type planes along the [111] direction. Without the knowledge of real structural information of doped systems, we have assumed the same structural parameters.

To check the magnetic instability, we calculate the Stoner exchange enhancement parameter *S*, defined as $S \equiv N(E_F)I_{XC}$ with I_{XC} denoting the intraatomic exchange-correlation integral. To investigate the superconducting properties of MgCNi₃ based on the rigid-ion approximation,¹¹⁾ the electron-phonon coupling constant λ_{ph} is evaluated by McMillan's formula¹²⁾

$$\lambda_{ph} = \sum_{\alpha} \frac{N(E_F)\langle I_{\alpha}^2 \rangle}{M_{\alpha}\langle \omega_{\alpha}^2 \rangle}, \quad (2.1)$$

where $\langle I_{\alpha}^2 \rangle$ is the average electron-ion interaction matrix element for the α -th ion, M_{α} is an ionic mass and $\langle \omega_{\alpha}^2 \rangle$ is the relevant phonon frequency. Since we have no information about phonon frequency, we instead use the average phonon frequency $\langle \omega^2 \rangle \simeq \Theta_D^2/2$, where Θ_D is the Debye temperature. Θ_D is adopted for 300 K and 400 K.

§3. Electronic structure of MgCNi₃

Total and partially projected local DOSs of MgCNi₃ are presented in Fig. 1. It is seen that Ni 3*d* and C 2*p* states are strongly hybridized. The peak near -7 eV and 4 eV correspond to σ bonding and σ^* antibonding states, respectively. On the other hand, the peak near -4 eV and E_F correspond to π bonding and π^* antibonding states, respectively. Because of the π^* antibonding states near E_F , the DOS is mainly composed by Ni 3*d* and C 2*p* states as shown in Table I. Especially, the contribution of Ni 3*d* states to the $N(E_F)$ is as much as 76%. Due to

* e-mail: jhshim@postech.ac.kr

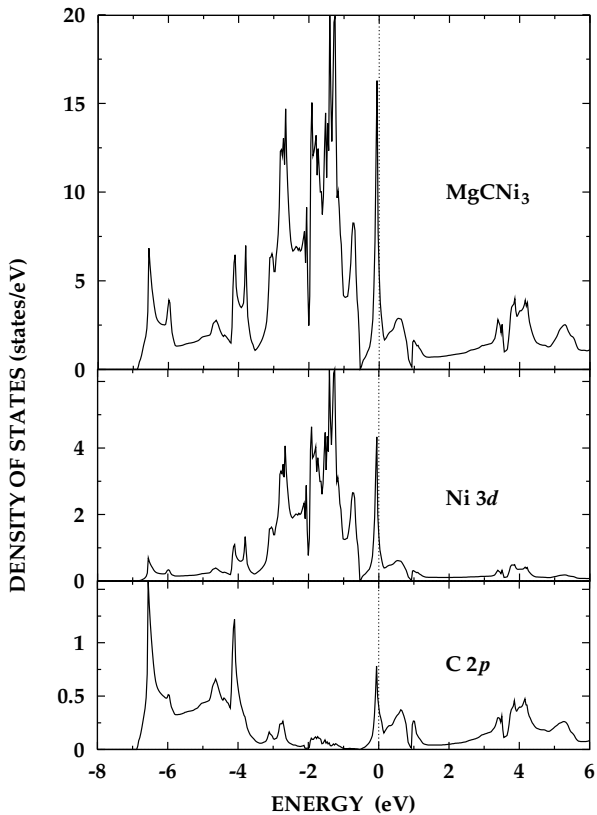


Fig. 1. The total and partially projected local DOS of MgCNi₃

very narrow and high peak in DOS located just below E_F , the system is expected to be perturbed much by small hole or electron doping. The Stoner parameter of $S = 0.64$ shows that this system is not magnetic, but it is expected to become magnetic by small hole doping in the rigid band scheme.

With the choice of $\Theta_D = 400$ K, one obtains $\lambda_{ph} = 0.77$. McMillan's T_c formula with an effective electron-electron interaction parameter $\mu^* = 0.13$ gives rise to $T_c = 11$ K, which are in reasonably agreement with experiment. The superconducting property will be also rapidly changed by hole or electron doping.

§4. Electronic structure of C-site and Mg-site doped MgCNi₃

To see the doping effect in a rigid band way, Mg-site or C-site doping would be more adequate rather than Ni-site doping. Ni-site doping would perturb electronic structure near E_F substantially due to the high contribution of doped element. We have examined quite a few doped

Table I. The calculated density of states at E_F (in states/eV) for MgCNi₃.

	<i>s</i>	<i>p</i>	<i>d</i>	<i>f</i>	Total
Mg	0.00	0.19	0.03		0.22
C	0.02	0.40	0.00		0.42
Ni	0.07	0.13	1.37	0.01	1.58

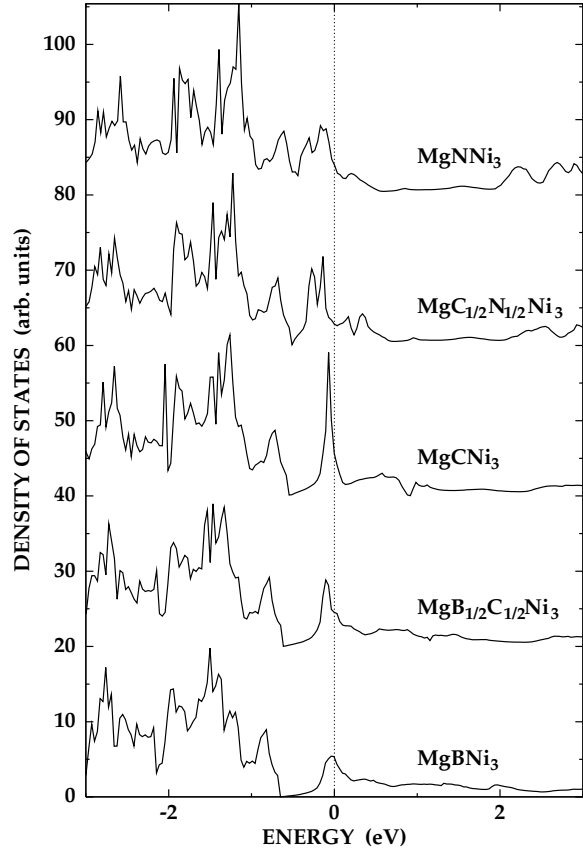


Fig. 2. Comparison of total DOSs by C-site doping

MgCNi₃ systems to see the doping effect systemically.

Firstly, C-site doping is studied by doping with B and N, which correspond to one hole and electron doping, respectively. As shown in Fig. 2, the effect of doping is mainly a variance of Fermi level, even though the shape of DOS near E_F is perturbed a little bit. Doping with B smears the DOS peak near E_F , because the upward shift of B 2*p* state induce the strong hybridization with Ni 3*d*. Although the Fermi level MgCNi₃ is just located at DOS peak, The DOS at E_F is not so high. By doping with N, the width of the DOS peak between E_F and 1.0 eV in MgCNi₃ is reduced so that the DOS shape near E_F is more perturbed. The DOS is not described by a systematic upward shift of the Fermi level.

Total DOS at E_F , $N(E_F)$, the Stoner parameter S , and the electron-phonon coupling constant λ_{ph} are compared for several doped systems in Table II. Contrary to the expectation in the rigid band scheme, $N(E_F)$ is high-

Table II. Comparison of total DOS at E_F , $N(E_F)$ (in states/eV), Stoner factor S , and electron phonon coupling constant λ_{ph} for $\Theta_D = 300$ K and 400 K by C-site doping.

	$N(E_F)$	S	$\lambda_{ph}(300K)$	$\lambda_{ph}(400K)$
MgBNi ₃	5.26	0.60	0.44	0.25
MgB _{1/2} C _{1/2} Ni ₃	4.61	0.53	0.78	1.11
MgCNi ₃	5.56	0.67	1.36	0.76
MgC _{1/2} N _{1/2} Ni ₃	2.84	0.34	0.59	0.33
MgNNi ₃	4.01	0.51	1.16	0.65

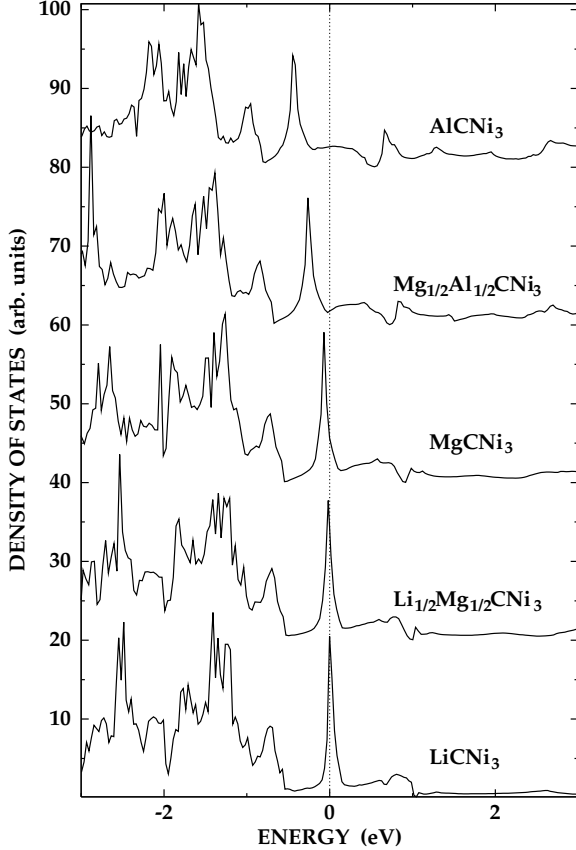


Fig. 3. Comparison of total DOSs by Mg-site doping

est in MgCNi_3 and do not show the systematic behavior. For all cases, the magnetic instability is not shown. From λ_{ph} , it is expected that electron or hole doping would suppress the superconductivity. But, MgNNi_3 is expected to have comparable T_c to MgCNi_3 , once synthesized successfully in the antiperovskite structure.

Mg-site doping is expected to be better described in the rigid band scheme, because the contribution of Mg to $N(E_F)$ is negligible in MgCNi_3 . We have performed the Mg-site doping with Li and Al, which have one less and one more electron. We have chosen Li as an effective hole doping element rather than Na, because the rigid band scheme works much better. As shown in Fig. 3, the doping results in only the shift of the Fermi level. The shape of DOS near E_F is well maintained.

Table III shows a systematic behavior of $N(E_F)$ by doping. By hole doping, $N(E_F)$ becomes much larger to produce the magnetic instability. Both LiCNi_3 and

$\text{Li}_{1/2}\text{Mg}_{1/2}\text{CNi}_3$ have ferromagnetic ground states with magnetic moments of $0.74 \mu_B$ and $0.82 \mu_B$. Therefore, Mg-site hole doping is expected to induce the transition from superconducting to magnetic instability. On the other hand, in the case of electron doping, $N(E_F)$ becomes much smaller than in MgCNi_3 , resulting in the suppression of superconductivity.

§5. Conclusion

We have investigated the electronic structure and superconducting property of MgCNi_3 . The π^* antibonding state of Ni $3d$ and C $2p$ states is located just below E_F . To explore the doping effect, we have considered the effective hole and electron dopings: at C-site by B and N, and at Mg-site by Li and Al. Mg-site doping is described better by the rigid band doping effect rather than C-site doping. Mg-site doping with Li is expected to show the transition from superconducting to magnetic ground state.

Acknowledgements

This work was supported by the KOSEF through the eSSC at POSTECH and in part by the BK21 Project. Helpful discussions with N. H. Hur are greatly appreciated.

-
- [1] D. Fruchart and E. F. Bertaut: J. Phys. Soc. Jap. **44** (1978) 781.
 - [2] K. Kamishima *et al.*: Phys. Rev. B **63** (2000) 024426.
 - [3] W. S. Kim, E. O. Chi, J. C. Kim, H. S. Choi, and N. H. Hur: Solid State Comm. **119** (2001) 507.
 - [4] T. He *et al.*: Nature **411** (2001) 54.
 - [5] M. A. Hayward *et al.*: Solid State Comm. **119** (2001) 491.
 - [6] S. B. Dugdale and T. Jarlborg: Phys. Rev. B **64** (2001) 100508(R).
 - [7] J. H. Shim, S. K. Kwon, and B. I. Min: Phys. Rev. B **64** (2001) 180510(R).
 - [8] D. J. Singh and I. I. Mazin: Phys. Rev. B **64** (2001) 140507(R).
 - [9] H. Rosner *et al.*: cond-mat/0106583 (2001).
 - [10] A. Szajek: J. Phys. Cond. Matt. **13** (2001) L595.
 - [11] G. D. Gaspari and B. L. Gyorffy: Phys. Rev. Lett. **28** (1972) 801.
 - [12] W. L. McMillan: Phys. Rev. **167** (1967) 331.

Table III. Comparison of total DOS at E_F , $N(E_F)$ (in states/eV), Stoner factor S , and electron phonon coupling constant λ_{ph} for $\Theta_D = 300$ K and 400 K by Mg-site doping.

	$N(E_F)$	S	$\lambda_{\text{ph}}(300\text{K})$	$\lambda_{\text{ph}}(400\text{K})$
LiCNi_3	20.43	2.43	2.86	1.61
$\text{Li}_{1/2}\text{Mg}_{1/2}\text{CNi}_3$	15.27	1.87	2.15	1.21
MgCNi_3	5.56	0.67	1.36	0.76
$\text{Mg}_{1/2}\text{Al}_{1/2}\text{CNi}_3$	1.81	0.21	0.39	0.22
AlCNi_3	2.61	0.29	0.52	0.29